ARTICLE

Flexible Thermochromic Window Based on Hybridized VO_2/Graphene

Hyeongkeun Kim,[†,▽] Yena Kim,[†,‡,▽] Keun Soo Kim,[§,▽] Hu Young Jeong,[⊥] A-Rang Jang,[∥] Seung Ho Han,[†] Dae Ho Yoon,[‡] Kwang S. Suh,[¶] Hyeon Suk Shin,[∥] TaeYoung Kim,[†,#,*] and Woo Seok Yang[†,*]

[†]Electronic Materials and Device Research Center, Korea Electronics Technology Institute, Gyeonggi-do 463-816, Korea, [‡]School of Advanced Materials Science and Engineering, Sungkyunkwan University, Suwon 440-746, Korea, [§]Department of Physics and Graphene Research Institute, Sejong University, Seoul 143-747, Korea, [⊥]UNIST Central Research Facilities and School of Mechanical & Advanced Materials Engineering and [∥]Interdisciplinary School of Green Energy, Low Dimensional Carbon Materials Center, and KIER-UNIST Advanced Center for Energy, Ulsan National Institute of Science and Technology (UNIST), Ulsan 689-798, Korea, [¶]Department of Materials Science and Engineering, Korea University, Seoul 136-701, Korea, and [#]Department of Mechanical Engineering and the Materials Science and Engineering Program, The University of Texas at Austin, Austin, Texas 78712, United States. [▽]These authors contributed equally to this work.

ABSTRACT Large-scale integration of vanadium dioxide (VO_2) on mechanically flexible substrates is critical to the realization of flexible smart window films that can respond to environmental temperatures to modulate light transmittance. Until now, the formation of highly crystalline and stoichiometric VO_2 on flexible substrate has not been demonstrated due to the high-temperature condition for VO_2 growth. Here, we demonstrate a VO_2-based thermochromic film with unprecedented mechanical flexibility by employing graphene as a versatile platform for VO_2. The graphene effectively functions as an atomically thin, flexible, yet robust support which enables the formation of stoichiometric VO_2 crystals with temperature-driven phase transition characteristics. The graphene-supported VO_2 was capable of being transferred to a plastic substrate, forming a new type of flexible thermochromic film. The flexible VO_2 films were then integrated into the mock-up house, exhibiting its efficient operation to reduce the in-house temperature under infrared irradiation. These results provide important progress for the fabrication of flexible thermochromic films for energy-saving windows.

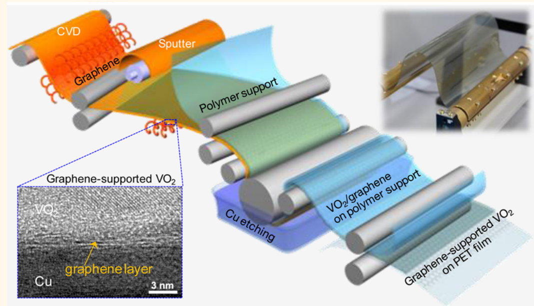

KEYWORDS: smart windows · vanadium dioxide · graphene · flexible thermochromic window · roll transfer

With growing demands for energy-saving technologies, vanadium dioxide (VO_2) is considered to be a promising candidate for energy-efficient smart windows.[1] VO_2 undergoes a fully reversible metal–insulator transition (MIT) at a temperature of 68 °C, coupled with a structural phase transition between monoclinic VO_2-(M) phase and rutile VO_2(R) phase.[2–5] The first-order phase transition in VO_2 is accompanied by a dramatic modification of the conductivity on several orders of magnitude and the corresponding optical transmittance; that is, the low-temperature insulating VO_2(M) is infrared-transparent, while the high-temperature metallic VO_2(R) is opaque in the infrared region. These unique features of VO_2 have sparked numerous potential applications in field-effect transistors, switches, sensors, and thermochromic coatings.[1,6–10]

The VO_2 phase with favorable transition characteristics has been synthesized by the techniques capable of precisely controlling oxygen partial pressure such as sputtering deposition,[10] pulsed laser deposition,[11] ion implantation,[12] and chemical vapor deposition (CVD),[13] which typically requires high-temperature processing. While the integration of VO_2 on mechanically flexible substrates is potentially promising for the realization of flexible thermochromic films as next-generation smart windows, high-temperature conditions required to form VO_2 limit the choice of substrates to rigid ones such as glass and sapphire.[14]

Toward the fabrication of flexible VO_2 films, several approaches may be taken into consideration. One is to grow VO_2 directly on flexible substrates, though it is technically hampered due to the lack of low-temperature VO_2 synthetic methods. In this sense, solution-based synthesis of VO_2 and its deposition on flexible substrate at low temperature may be a good option for the low-cost and large-area fabrication.[15–21] However, flexible thermochromic films with

* Address correspondence to taeykim@utexas.edu, wsyang@keti.re.kr.

Received for review January 23, 2013 and accepted June 11, 2013.

Published online June 11, 2013
10.1021/nn400358x

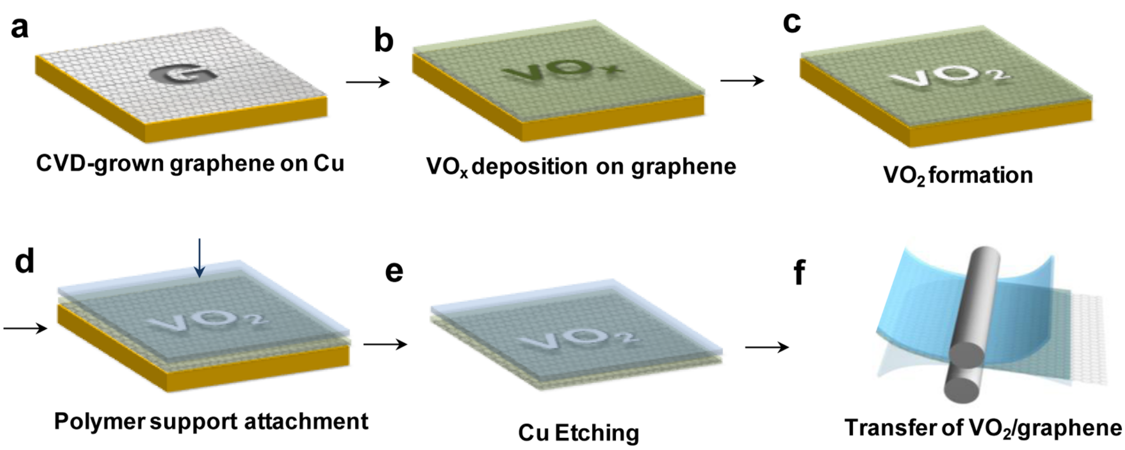

Figure 1. Schematic of the fabrication of graphene-supported flexible VO_2 film. (a) Synthesis of graphene on a Cu foil using the chemical vapor deposition (CVD) method. (b) VO_x deposition on graphene by RF sputtering. (c) Postannealing for VO_2 formation. (d) Lamination of VO_2/graphene/Cu with thermal release tape etching of underlying Cu foil. (f) Transfer of graphene-supported VO_2 onto a flexible substrate.

VO_2 particulates prepared through solution-based synthesis often suffer from their modest quality or durability with the metal−insulator phase being often smeared out.[17−21]

Another option is to synthesize highly crystalline VO_2 on the rigid substrates using conventional high-temperature methods and transfer it onto flexible substrates, which may provide a new pathway to fabricate VO_2-based thermochromic films on flexible substrates. Here, our approach is based on the utilization of graphene as an atomically thin two-dimensional support for VO_2. With key advantages such as high optical transmission, thermal stability, and mechanical flexibility,[16,22−24] graphene may be an ideal support for the formation of high-quality VO_2. We further demonstrate that graphene-supported VO_2 films can be easily transferred to flexible substrates, taking advantage of well-established graphene transfer techniques.[25,26] The fabricated VO_2-based film is mechanically flexible, while maintaining a fully reversible phase transition feature with good optical switching efficiencies. To our knowledge, this is the first demonstration of a method that allows for the deposition of VO_2 on a plastic substrate, thereby producing a flexible VO_2-based thermochromic film.

RESULTS AND DISCUSSION

The procedure for the preparation of flexible VO_2-based thermochromic film is outlined in Figure 1. In the first step, we grew single- or few-layer graphene on copper (Cu) foils by the CVD method (Supporting Information, Figure S1)[25−27] and used them (graphene/Cu) as a support for VO_x crystals. Amorphous and substoichiometric VO_x (∼40 nm thick) was deposited onto graphene by RF magnetron sputtering of vanadium metal. Following the VO_x deposition, a VO_x/graphene/Cu was then annealed at 500 °C with O_2 flow of 50 sccm to render the film crystalline and near-stoichiometric VO_2 (Supporting Information, Figure S1). As-produced graphene-supported VO_2 on Cu foil (VO_2/graphene/Cu) was then attached to a thermal release tape and floated on 0.1 M of ammonium persulfate solution to etch Cu foils. After several washes with deionized water, graphene-supported VO_2 (VO_2/graphene) on thermal release tape was laminated with poly(ethyleneterephthalate) (PET) film using rollers and exposed to mild heat (120 °C), through which the VO_2/graphene was transferred to PET film (Supporting Information, Figure S2).[25] An alternative transfer process with the use of polymer backing film (*e.g.*, poly(methylmethacrylate), PMMA) was also possible as follows: VO_2/graphene/Cu was coated with a thin film of PMMA; the underlying Cu was etched; VO_2/graphene was transferred to either flexible or rigid substrates.[25−27] Our approach to use graphene as a support for VO_2 growth and a transferring medium allows for the fabrication of large-area (up to ∼8 in.) and flexible graphene-supported VO_2 film (VO_2/graphene/PET), as shown in Supporting Information Figure S2. We note that, in a control experiment where VO_2 is directly deposited on graphene-free Cu foil (VO_2/Cu), transfer of VO_2 to PET substrates was unsuccessful (Supporting Information, Figure S2), which is an indication that graphene is a key element to transfer VO_2 to the PET substrate.

The morphology and structure of VO_2 crystals on both graphene support and graphene-free Cu substrate were examined using high-resolution transmission electron microscopy (TEM) (Figure 2). Cross-sectional TEM image of graphene-free VO_x on Cu substrate (VO_x/Cu) (Figure 2a) revealed that polycrystalline VO_x nanostructures with sizes ∼100 nm are rather loosely distributed as islands on the Cu substrate. These sparsely distributed VO_x islands on the Cu substrate were difficult to transfer to PET substrates as described earlier, presumably due to loosely bound VO_x island morphology. The fast Fourier transform

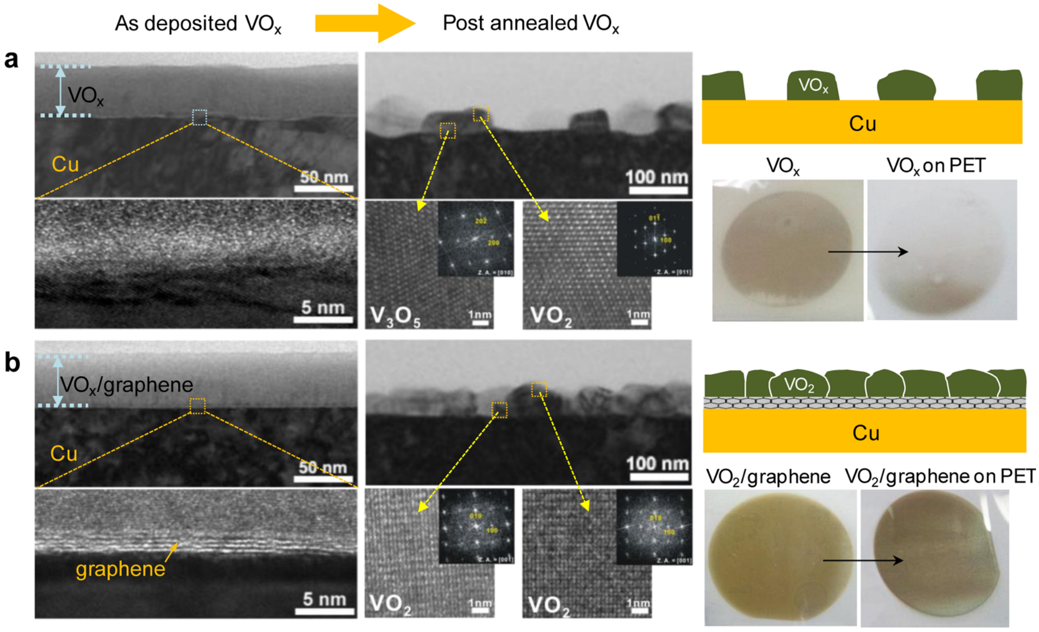

Figure 2. Structural characterization of the graphene-supported VO_2. (a) High-resolution transmission electron microscopy (HR-TEM) of the cross section of as-deposited and postannealed VO_x on graphene-free copper substrate (VO_x/Cu). The postannealing of graphene-free VO_x led to the formation of sparsely distributed VO_x crystals. (b) HR-TEM of the cross section of as-deposited and postannealed graphene-supported VO_2 on copper (VO_2/graphene/Cu). The postannealing of graphene-supported VO_x afforded the formation of densely interlinked VO_2 crystals. The FFT patterns after postannealing were indexed to an identical VO_2 crystalline phase. Photographs show VO_2/graphene laminated with thermal release tape (left) and VO_2/graphene transferred to PET film (right).

(FFT) patterns were taken from two different spots (top and bottom region) to investigate the crystal structure of the graphene-free VO_x island along the thickness direction. FFT analysis shows that the crystalline phase of VO_x in these two spots can be indexed to VO_2 and V_3O_5, indicating a mixture of vanadium oxides with a different oxidation state. In contrast, imaging of the cross sections of graphene-supported VO_2 on Cu (VO_2/graphene/Cu) shows contiguously interlinked VO_2 nanocrystals on graphene support (Figure 2b).[28] In the magnified TEM image of the VO_2/graphene/Cu sample, the graphene of single to triple layers is also clearly visible between the VO_2 and Cu layer, with the average interlayer spacing of ~0.34 nm (Supporting Information, Figure S3). The FFT patterns taken from two randomly selected spots indicate a coherent crystalline structure of graphene-supported VO_2 which is indexed to the VO_2(M). Although further structural and chemical analysis of graphene-supported VO_2 crystals with X-ray diffraction (XRD) and X-ray photoelectron spectroscopy (XPS) showed that it is not composed of pure VO_2 crystals and rather contains a trace amount of other VO_x compounds with different oxidation state (Supporting Information, Figures S4 and S6); this result along with other analysis data suggests that the VO_2 phase was dominantly formed on graphene support. In addition, it is evident that graphene serves to aid the formation of densely interlinked VO_2 nanocrystals and therefore permits the straightforward transfer of VO_2 to PET film.

For further characterization, the structures of VO_2 and graphene were determined from Raman spectroscopy (Figure 3). In contrast to the graphene-free VO_x sample (Figure 3a, black line), the graphene-supported VO_2 (transferred to SiO_2/Si substrate, VO_2/graphene/SiO_2) (Figure 3a, red line) shows a typical Raman feature of CVD-grown graphene: I_G/I_{2D} of 0.62 and a symmetric 2D band centered at ~2694 cm^{-1} with full width at half-maximum (fwhm) of ~38 cm^{-1}.[25,26] We note that there is a slight increase in the D-peak (1350 cm^{-1}) intensity of graphene after VO_2 formation, whereas the as-synthesized graphene shows a minimal D-peak indicating a negligibly small portion of structural defects (Supporting Information, Figure S5).[25] The increase in D-peak was attributed to high-temperature oxidation of graphene during postannealing of VO_x at 500 °C under O_2 flowing (Supporting Information, Figure S5)[28−30] (see Supporting Information for further Raman analysis).

The Raman features for VO_2 were displayed in Figure 3b. Both graphene-free (VO_x/Cu) and graphene-supported VO_2 (VO_2/graphene/Cu) show several peaks (144, 194, 226, 262, 310, 342, 389, 445, 500, and 615 cm^{-1}) corresponding to the characteristic vibration modes assigned to monoclinic VO_2.[31] However, the Raman peaks of VO_2/graphene/Cu are more pronounced as compared with those of VO_x/Cu. This is likely due to the intensified Raman signals originating from the dense VO_2 distribution on the graphene support.

To gain more insights into the structural phase transition of graphene-supported VO_2 film, the evolution of Raman peaks was monitored as a function of temperature (Figure 3c). With increasing temperature,

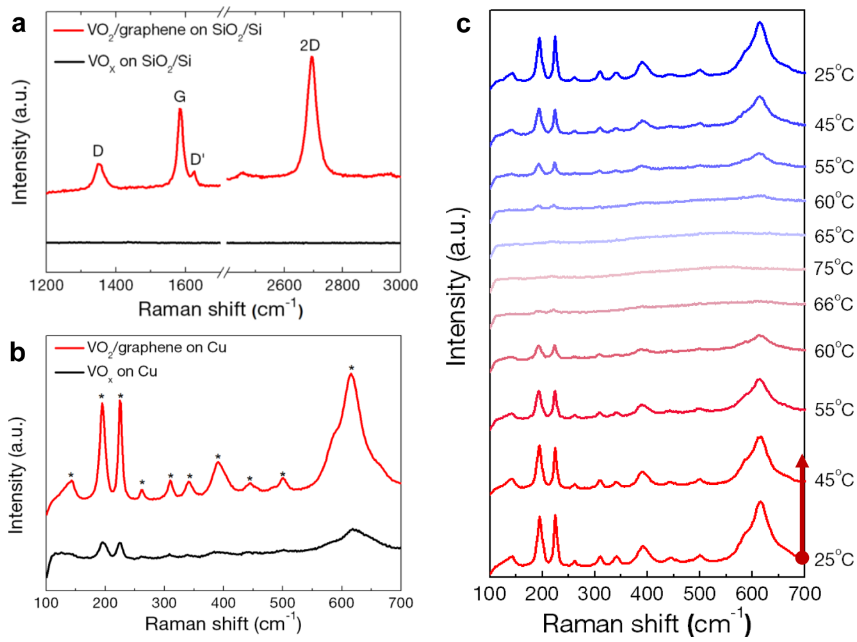

Figure 3. Raman spectral analysis of the graphene-supported VO_2. (a,b) Raman spectra (excited by 532 nm laser) of graphene-supported VO_2 in comparison with graphene-free VO_x. (c) Sequential Raman spectra of graphene-supported VO_2 on heating and cooling cycle.

the characteristic Raman peaks of monoclinic VO_2 diminish through intermediate phase coexistence regimes and then completely disappear at ∼70 °C, indicating a structural transition of low-temperature VO_2(M) into the high-temperature VO_2(R) phase.[30,32] With decreasing temperature, the monoclinic signature reappears, showing the reverse transition from VO_2(R) to VO_2(M) phase. Therefore, the graphene-supported VO_2 displays the prototypical signatures of a reversible first-order transition.

The chemical compositions of VO_2 were probed by X-ray photoelectron spectroscopy (XPS) (Figure 4). The XPS core-level spectra of $V2p_{3/2}$ and O1s for the graphene-supported and graphene-free VO_x on copper are shown in Figure 4a. For the graphene-supported VO_2 on copper (VO_2/graphene/Cu), the $V2p_{3/2}$ spectrum displays a peak with a maximum at 516.6 eV that can be attributed to a 4+ oxidation state of vanadium.[33] However, the $V2p_{3/2}$ spectrum of the graphene-free VO_x (VO_x/Cu) differs in shift to lower binding energy, indicating that V^{+5} is the primary oxidation state. The measurement of depth-dependent O/V ratio also shows that the stoichiometry for graphene-supported VO_2 is nearly uniform across the VO_2 film thickness, whereas nonstoichiometry was observed for VO_x/Cu sample (Figure 4b). These results indicate that VO_x film directly grown on Cu has a formula significantly deviating from VO_2, which is consistent with the result from TEM and XRD measurement. In addition, graphene-free VO_x shows a significant amount of Cu contaminants which likely migrate from the Cu foil into the VO_x layer during a high-temperature annealing process, while graphene-supported VO_2 shows a negligible level of Cu contents in the VO_2 layer. This result indicates that graphene serves as a diffusion barrier providing a physical separation between the Cu and VO_x layers.[34]

In addition, the graphene layer plays a role in suppressing oxidation of the Cu layer as evidenced by the comparison of Cu2p XPS spectra (Figure 4c). The XPS spectra of Cu foils show two main Cu peaks at binding energies of 932.3 and 952.3 eV corresponding to $Cu2p_{3/2}$ and $Cu2p_{1/2}$, respectively.[34] However, the VO_x/Cu sample shows multiple Cu peaks that can be assigned to different copper oxides, such as Cu_2O (932.5 and 952.1 eV), CuO (934.3 and 953.6 eV), and $Cu(OH)_2$ (935.4 and 954.3 eV), indicating that Cu was significantly oxidized during the postannealing process of the VO_x layer.[34] Hence, it can be concluded that graphene acts as a barrier for interdiffusion (Figure 4b) between Cu and VO_x, protecting the underlying Cu substrate from oxidation and the top VO_x layer from contamination, as illustrated in the inset of Figure 4c.

To identify the thermochromic properties of the graphene-supported VO_2 (VO_2/graphene) films, we measured temperature-dependent optical transmittance of the films (Figure 5). A VO_2/graphene film shows an optical transparency of 65.4% at the 550 nm wavelength and displays a typical thermochromic behavior with an abrupt change in the infrared region when the transmittance of the film was measured at 25 and 100 °C (Figure 5b).

The temperature-dependent optical transmission (at the wavelength of 2500 nm) and thermal hysteresis loop of VO_2/graphene/PET film are shown in Figure 5c. Through heating and cooling cycles, the VO_2/graphene/PET film undergoes a reversible phase transition with a NIR switching efficiency of ΔT_r = 53% at λ = 2500 nm and shows the characteristic hysteretic

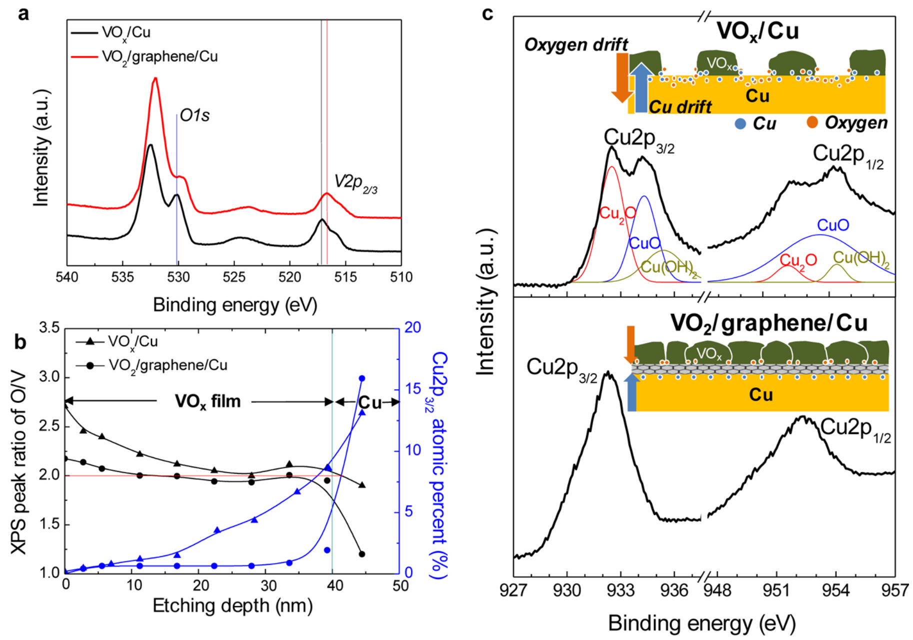

Figure 4. X-ray photoelectron spectroscopy (XPS) spectra of the graphene-supported VO_2. (a) XPS spectra of the graphene-supported VO_2 (VO_2/graphene/Cu) and the graphene-free VO_x films (VO_x/Cu). (b) XPS depth profile showing the variation in the O/V peak ratio and the migration of copper contaminant. (c) XPS core-level Cu2p spectra of VO_x/Cu (top panel) and VO_2/graphene/Cu (bottom panel).

behavior with ΔT = 9.8 °C. While the hysteresis is relevant to the multidomain VO_2 structure, nanosized VO_2 crystals, and other parameters,[14,35,36] a relatively large hysteresis observed for VO_2/graphene/PET film is partially attributed to the presence of other VO_x phases such as V_2O_5 and V_3O_5.[37,38,41] Graphene-supported VO_2 shows two distinct transition temperatures of 65.4 °C on heating and 56.6 °C on cooling, giving the transition temperature T_c = 61 °C from $T_c = (T_{heating} + T_{cooling})/2$. This indicates that graphene-supported VO_2 showed a transition temperature lower than those measured for stoichiometric VO_2 single crystals.[1−6,14] In general, depression of the phase transition in VO_2 can have several origins: doping with other transition metals, strain, structural ordering, and scaling to nanoscale dimensions.[13−15,39−41] As the VO_2 preparation method described here does not use any other transition metals, we attribute depression of the phase transition temperature to the effect of graphene support on reducing VO_2 crystal size to nanoscale. In addition, with the high thermal conductivity reported for the graphene, the efficient heat transfer from graphene to VO_2 may account for the depression of MIT temperature. Further work is underway to further understand the effect of underlying graphene on the phase transition characteristics of the graphene-supported VO_2.

We also evaluated the bending stability of the VO_2/graphene/PET film by measuring resistance change ($\Delta R/R_0$) as a function of strain (inset of Figure 5d). A minimal resistance change over a strain ranging from 1 to 6% suggests that graphene-supported VO_2 film is mechanically flexible without any serious mechanical damage or fracture of the film.[25,42] It is noted that we measured the resistance of the VO_2/graphene hybrid film upon bending, and the measured values reflect the combined resistance of VO_2 and graphene layers. For the repetitive bending cycling test, the flexible VO_2/graphene/PET film was tested on an automated bending machine. As shown in Figure 5d, the $\Delta R/R_0$ values of the film were maintained when bent over 1000 times, indicating an excellent flexibility of the film. These results also suggest that there were no significant changes in the structure of graphene-supported VO_2 films and the adhesion at the interface between graphene support and VO_2 crystals.

The above results suggest that the graphene-supported VO_2 film can be readily applicable to a new type of energy-efficient flexible film that automatically limits the optical transmission when the temperature reaches a defined value. As a prototype, we fabricated a model house with VO_2/graphene/PET thermochromic windows (Figure 5a) and evaluated its performance by measuring inner-house temperature changes after irradiation under an artificial solar lamp (Figure 5e)[43] (Supporting Information, Figure S6). As a control experiment, a window based on VO_2-free graphene/PET film was also tested. In the first 5 min of solar irradiation, the temperature is below the transition temperature of VO_2, and thus solar irradiation can be transmitted by the two windows, giving almost the same inner-house temperature. However, as the VO_2 reached the transition temperature, the temperature difference between the two inner rooms was about 5.8 °C, indicating that a significant amount of irradiation was blocked by the graphene/VO_2 window.

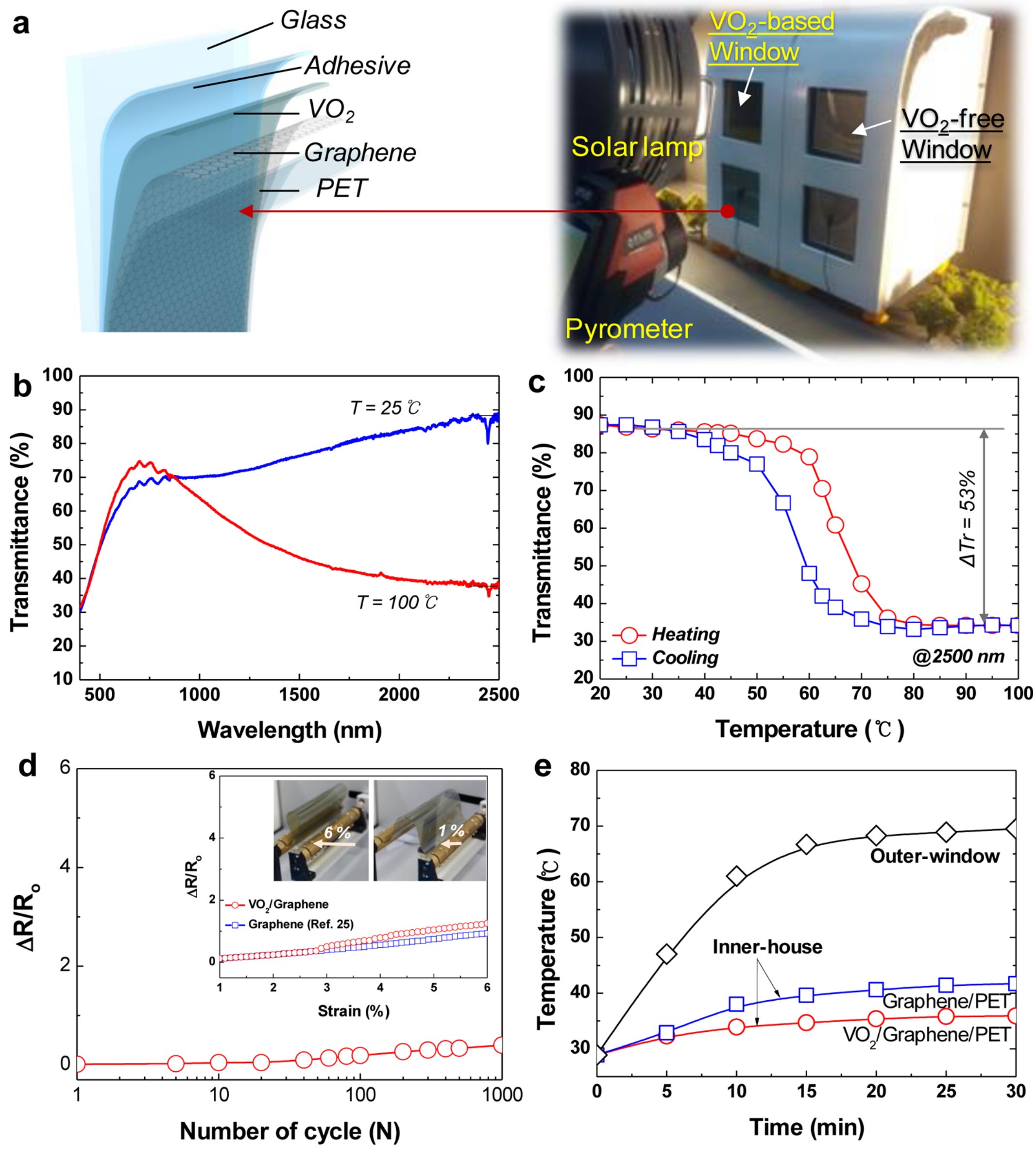

Figure 5. Thermochromic properties of the graphene-supported VO_2 film. (a) Structure of the graphene-supported VO_2 film. Photograph of model house equipped with VO_2-based window (VO_2/graphene/PET film) and VO_2-free window (graphene/PET film). (b) Transmission spectra of the VO_2/graphene/PET film taken at temperatures of 25 and 100 °C. (c) Temperature-dependent optical transmission (at λ = 2500 nm) of VO_2/graphene/PET film. (d) Resistance change of a VO_2/graphene/PET film against repeated bending cycle. The inset shows resistance changes as a function of strain. (e) Temperature change of model house upon solar irradiation as a function of exposure time.

CONCLUSION

We present a fabrication method of mechanically flexible VO_2-based thermochromic films. Graphene was employed to provide an atomically thin two-dimensional support for the growth of high-quality VO_2 and function as a shuttle to transfer the VO_2 layer to a flexible substrate. Large-area graphene-supported VO_2 films exhibited mechanical flexibility while preserving its characteristic phase transition behavior with efficient switching behavior and lowered phase transition temperatures. The fabricated VO_2/graphene hybrid films were integrated into the model house and shown to reduce the in-house temperature efficiently, demonstrating its potential as energy-saving smart window films.

METHODS

Preparation of Graphene-Supported VO_2 Films. Single-layer graphene was grown on copper foils using a CVD method. First, the Cu foil (99.8%, Alfa-Aesar, item no. 13382) was loaded into a quartz tube of the CVD system and annealed at 1000 °C under 90 mTorr with flowing 10 sccm of H_2 for 60 min to enlarge the single-crystalline graphene size of the Cu foil. The growth was initiated by flowing reaction gas mixtures (CH_4/H_2 = 15:10 sccm) under 560 mTorr for 25 min, followed by rapidly cooling the sample to room temperature (10 °C min^{-1}) with flowing H_2 under 90 mTorr.[25,26]

The VO_x thin layer was prepared on the graphene/Cu and bare Cu substrates in a RF magnetron sputtering system. Sputtering was carried out with a water-cooled vanadium metal target (100 mm diameter, purity 99.99%). Prior to the deposition of VO_x, the substrate was presputtered by Ar ion plasma to eliminate contamination. Deposition was carried out at room temperature under argon (97 sccm) and oxygen (3 sccm) flowing for 40 min, and RF power of 300 W and a total pressure of 0.63 Pa were maintained during the deposition. For VO_2 single-phase formation, postannealing of VO_x thin film on the graphene/Cu substrate was performed at 500 °C for 30 min under high vacuum of $\sim 10^{-5}$ Pa with 50 sccm flowing O_2.

For the transfer of the film onto the PET substrate, the as-produced VO_2/graphene/Cu film was attached to a thermal release tape (Nitto Denko) by applying a pressure of ~0.2 MPa using a roller. After etching the Cu layer and rinsing the residual etchant using deionized water, the VO_2/graphene on thermal release tape was laminated with PET film and exposed to mild heat (120 °C). Some of the VO_2/graphene/Cu film sample was coated with a thin layer of poly(methylmethacrylate) (PMMA), and then the underlying Cu foil was etched away in aqueous 0.1 M ammonium persulfate solution. After several washes with deionized water, the PMMA-backed VO_2/graphene was transferred onto SiO_2 (300 nm)/Si substrates.[25]

Characterization. Morphologies of the VO_2 film were examined by field-emission scanning electron microscope (FE-SEM, JSM-6490) and transmission electron microscopy (TEM, JEM-2100F operated at 200 kV). Phase identification was performed using X-ray diffraction (XRD, Bruker D8 Advance with Cu Kα radiation, λ = 1.54056 Å). Raman spectrum was obtained using the Renishaw inVia Raman microscope spectrometer with 514 nm wavelength excitation. X-ray photoelectron spectroscopy (XPS, Sigma Probe ThermoVG) was performed using monochromatic Al Kα radiation. Thermochromic switching characteristics were monitored on a UV–vis–NIR spectrophotometer (JASCO V-670) equipped with a film heating unit in the wavelength range of 300–2500 nm. The temperature was measured using a thermocouple in contact with films and was controlled through a temperature-controlling unit. Hysteresis loop was measured by collecting transmittance of films at a fixed wavelength (2500 nm) at a temperature interval of 9.8 °C. A model house (25 × 20 × 30 cm^3) was made of boards measuring 10 mm in thickness, and VO_2/graphene/PET film was attached to the front windows (12 × 12 cm^2). An artificial solar lamp was used as the heat source to simulate solar radiation and positioned at a distance of 40 cm from the smart window.[43] Pyrometer was used to measure the temperature of the window, and two thermocouples were installed inside each house to monitor inner-house temperatures.

Conflict of Interest: The authors declare no competing financial interest.

Acknowledgment. This work was supported by Technology Innovation Program (No. 10044410, Commercialization of flexible touch panels based on 900 × 1600 mm^2 large, less than 1 nm thick graphene film synthesis technique) funded by the Ministry of Trade, Industry and Energy, Energy Efficiency & Resources of the Korea Institute of Energy Technology Evaluation and Planning (KETEP) (No. 2012T100201723) funded by the Korea government Ministry of Knowledge Economy, Priority Research Centers Program (GT-SWS-11-01-004-0, Global Top Project; The Eco-Innovation Project) funded by Korea Ministry of Environment, the Global Frontier Research Program through the National Research Foundation (NRF) (No. 2011-0031630, from the Center for Advanced Soft Electronics) funded by the Ministry of Education, Science and Technology (MEST) of Korea, and K.S.K. was supported by Priority Research Centers Program (2010-0020207) through the NRF funded by the Ministry of Education, Basic Science Program (2011-0029645), Nano Material Technology Development Program through the NRF funded by the Ministry of Science, ICT and Future Planning (2012M3A7B4049888) and TJ Park Science Fellowship of POSCO TJ Park Foundation. TEM studies were performed at UNIST Central Research Facilities (UCRF) at UNIST, and we thank Prof. S.M. Ryu (Kyung Hee U.) and Prof. E.J. Choi (The U. of Seoul) for helpful comments.

Supporting Information Available: Experimental methods and additional results. This material is available free of charge *via* the Internet at http://pubs.acs.org.

REFERENCES AND NOTES

1. Morin, F. J. Oxides Which Show a Metal-to-Insulator Transition at the Neel Temperature. *Phys. Rev. Lett.* **1959**, *3*, 34–36.
2. Wentzcovitch, R. M.; Schulz, W. W.; Allen, P. B. VO_2: Peierls or Mott-Hubbard? View from Band Theory. *Phys. Rev. Lett.* **1994**, *72*, 3389–3392.
3. Cavalleri, A.; Dekorsy, T.; Chong, H. H. W.; Kieffer, J. C.; Schoenlein, R. W. Evidence for a Structurally-Driven Insulator-to-Metal Transition in VO_2: A View from the Ultrafast Timescale. *Phys. Rev. B* **2004**, *70*, 161102.
4. Kim, T.-H.; Angst, M.; Hu, B.; Jin, R.; Zhang, X.-G.; Wendelken, J. F.; Plummer, E. W.; Li, A.-P. Imaging and Manipulation of the Competing Electronic Phases near the Mott Metal-Insulator Transition. *Proc. Natl. Acad. Sci. U.S.A.* **2010**, *107*, 5272–5275.
5. Wu, C.; Wei, H.; Ning, B.; Xie, Y. New Vanadium Oxide Nanostructures: Controlled Synthesis and Their Smart Electrical Switching Properties. *Adv. Mater.* **2010**, *22*, 1972–1976.
6. Wu, J.; Gu, Q.; Guiton, B. S.; de Leon, N. P.; Ouyang, L.; Park, H. Strain-Induced Self Organization of Metal–Insulator Domains in Single-Crystalline VO_2 Nanobeams. *Nano Lett.* **2006**, *6*, 2313–2317.
7. Qazilbash, M. M.; Brehm, M.; Chae, B.-G.; Ho, P.-C.; Andreev, G. O.; Kim, B.-J.; Yun, S. J.; Balatsky, A. V.; Maple, M. B.; Keilmann, F.; *et al.* Mott Transition in VO_2 Revealed by Infrared Spectroscopy and Nano-Imaging. *Science* **2007**, *318*, 1750–1753.
8. Kübler, C.; Ehrke, H.; Huber, R.; Lopez, R.; Halabica, A.; Haglund, R. F., Jr.; Leitenstorfer, A. Coherent Structural Dynamics and Electronic Correlations during an Ultrafast Insulator-to-Metal Phase Transition in VO_2. *Phys. Rev. Lett.* **2007**, *99*, 116401.
9. Strelcov, E.; Lilach, Y.; Kolmakov, A. Gas Sensor Based on Metal–Insulator Transition in VO_2 Nanowire Thermistor. *Nano Lett.* **2009**, *9*, 2322–2326.
10. Appavoo, K.; Haglund, R. F., Jr. Detecting Nanoscale Size Dependence in VO_2 Phase Transition Using a Split-Ring Resonator Metamaterial. *Nano Lett.* **2011**, *11*, 1025–1031.
11. Kim, D. H.; Kwok, H. S. Pulsed Laser Deposition of VO_2 Thin Films. *Appl. Phys. Lett.* **1994**, *65*, 3188–3190.
12. Gea, L. A.; Boatner, L. A. Optical Switching of Coherent VO_2 Precipitates Formed in Sapphire by Ion Implantation and Annealing. *Appl. Phys. Lett.* **1996**, *68*, 3081–3083.
13. Manning, T. D.; Parkin, I. P.; Pemble, M.; Sheel, D.; Vernardou, D. Intelligent Window Coatings: Atmospheric Pressure Chemical Vapor Deposition of Tungsten-Doped Vanadium Dioxide. *Chem. Mater.* **2004**, *16*, 744–749.
14. Parkin, I. P.; Manning, T. D. Intelligent Thermochromic Windows. *J. Chem. Educ.* **2006**, *83*, 393–400.
15. Gao, Y.; Luo, H.; Zhang, Z.; Kang, L.; Chen, Z.; Du, J.; Kanehira, M.; Cao, C. Nanoceramic VO_2 Thermochromic Smart Glass: A Review on Progress in Solution Processing. *Nano Energy* **2012**, *1*, 221–246.
16. Gao, Y.; Wang, S.; Kang, L.; Chen, Z.; Du, J.; Liu, X.; Luo, H.; Kanehira, M. VO_2-Sb:SnO_2 Composite Thermochromic Smart Glass Foil Energy. *Energy Environ. Sci.* **2012**, *5*, 8234–8237.
17. Chae, B.-G.; Kim, H.-T.; Yun, S.-J.; Kim, B.-J.; Lee, Y.-W.; Kang, K.-Y. Comparative Analysis of VO_2 Thin Films Prepared on Sapphire and SiO_2/Si Substrates by the Sol–Gel Process. *Jpn. J. Appl. Phys.* **2007**, *46*, 738–743.
18. Li, S.-Y.; Niklasson, G. A.; Granqvist, C. G. Thermochromic Fenestration with VO_2-Based Materials: Three Challenges and How They Can Be Met. *Thin Solid Films* **2012**, *520*, 3823–3828.
19. Chae, B. G.; Kim, H. T.; Yun, S. J. Characteristics of W- and Ti-Doped VO_2 Thin Films Prepared by Sol–Gel Method. *Electrochem. Solid Lett.* **2008**, *11*, D53–D55.

20. Chae, B. G.; Kim, H. T. Effects of W Doping on the Metal−Insulator Transition in Vanadium Dioxide Film. *Physica B* **2010**, *405*, 663–667.
21. Takahashi, I.; Hibino, M.; Kudo, T. Thermochromic $V_{1-x}W_xO_2$ Thin Films Prepared by Wet Coating Using Polyvanadate Solutions. *Jpn. J. Appl. Phys.* **1996**, *35*, L438–L440.
22. Geim, A. K.; Novoselov, K. S. The Rise of Graphene. *Nat. Mater.* **2007**, *6*, 183–191.
23. Lee, C.; Wei, X.; Kysar, J. W.; Hone, J. Measurement of the Elastic Properties and Intrinsic Strength of Monolayer Graphene. *Science* **2008**, *321*, 385–388.
24. Nair, R. R.; Blake, P.; Grigorenko, A. N.; Novoselov, K. S.; Booth, T. J.; Stauber, T.; Peres, N. M. R.; Geim, A. K. Fine Structure Constant Defines Visual Transparency of Graphene. *Science* **2008**, *320*, 1308.
25. Bae, S.; Kim, H.; Lee, Y.; Xu, X.; Park, J.-S.; Zheng, Y.; Balakrishnan, J.; Lei, T.; Kim, H. R.; Song, Y. I.; *et al.* Roll-to-Roll Production of 30-Inch Graphene Films for Transparent Electrodes. *Nat. Nanotechnol.* **2010**, *5*, 574–578.
26. Kang, J.; Hwang, S.; Kim, J. H.; Kim, M. H.; Ryu, J.; Seo, S. J.; Hong, B. H.; Kim, M. K.; Choi, J.-B. Efficient Transfer of Large-Area Graphene Films onto Rigid Substrates by Hot Pressing. *ACS Nano* **2012**, *6*, 5360–5365.
27. Li, X.; Cai, W.; An, J.; Kim, S.; Nah, J.; Yang, D.; Piner, R.; Velamakanni, A.; Jung, I.; Tutuc, E.; *et al.* Large-Area Synthesis of High-Quality and Uniform Graphene Films on Copper Foils. *Science* **2009**, *324*, 1312–1314.
28. Kim, Y.-J.; Yoo, H.; Lee, C.-H.; Park, J. B.; Baek, H.; Kim, M.; Yi, G.-C. Position- and Morphology-Controlled ZnO Nanostructures Grown on Graphene Layers. *Adv. Mater.* **2012**, *24*, 5565–5569.
29. Ferrari, A. C.; Meyer, J. C.; Scardaci, V.; Casiraghi, C.; Lazzeri, M.; Mauri, F.; Piscanec, S.; Jiang, D.; Novoselov, K. S.; Roth, S.; *et al.* Raman Spectrum of Graphene and Graphene Layers. *Phys. Rev. Lett.* **2006**, *97*, 187401.
30. Ryu, S.; Liu, L.; Berciaud, S.; Yu, Y.-J.; Liu, H.; Kim, P.; Flynn, G. W.; Brus, L. E. Atmospheric Oxygen Binding and Hole Doping in Deformed Graphene on a SiO_2 Substrate. *Nano Lett.* **2010**, *10*, 4944–4951.
31. Jones, A. C.; Berweger, S.; Wei, J.; Cobden, D.; Raschke, M. B. Nano-optical Investigations of the Metal-Insulator Phase Behavior of Individual VO_2 Microcrystals. *Nano Lett.* **2010**, *10*, 1574–1581.
32. Kim, B.-J.; Lee, Y. W.; Chae, B.-G.; Yun, S. J.; Oh, S.-Y.; Kim, H.-T.; Lim, Y.-S. Temperature Dependence of the First-Order Metal-Insulator Transition in VO_2 and Programmable Critical Temperature Sensor. *Appl. Phys. Lett.* **2007**, *90*, 023515.
33. Yang, Z.; Ramanathan, S. Direct Measurement of Compositional Complexity-Induced Electronic Inhomogeneity in VO_2 Thin Films Grown on Gate Dielectrics. *Appl. Phys. Lett.* **2011**, *98*, 192113.
34. Chen, S.; Brown, L.; Levendorf, M.; Cai, W.; Ju, S.-Y.; Edgeworth, J.; Li, X.; Magnuson, C. W.; Velamakanni, A.; Piner, R. D.; *et al.* Oxidation Resistance of Graphene-Coated Cu and Cu/Ni Alloy. *ACS Nano* **2011**, *5*, 1321–1327.
35. Zhang, Z.; Gao, Y.; Luo, H.; Kang, L.; Chen, Z.; Du, J.; Kanehira, M.; Zhang, Y.; Wang, Z. L. Solution-Based Fabrication of Vanadium Dioxide on $F:SnO_2$ Substrates with Largely Enhanced Thermochromism and Low-Emissivity for Energy-Saving Applications. *Energy Environ. Sci.* **2011**, *4*, 4290–4297.
36. Xu, G.; Huang, C.-M.; Tazawa, M.; Jin, P.; Chen, D.-M.; Miao, L. Electron Injection Assisted Phase Transition in a Nano-Au-VO_2 Junction. *Appl. Phys. Lett.* **2008**, *93*, 061911.
37. Eiji, K.; Jeremy, A. T. Effects of Microstructures and Nonstoichiometry on Electrical Properties of Vanadium Dioxide Films. *J. Vac. Sci. Technol., A* **1989**, *7*, 1314–1317.
38. Zheng, Y.; Shriram, R. Direct Measurement of Compositional Complexity-Induced Electronic Inhomogeneity in VO_2 Thin Films Grown on Gate Dielectrics. *Appl. Phys. Lett.* **2011**, *98*, 192113.
39. Gao, Y.; Wang, S.; Luo, H.; Dai, L.; Cao, C.; Liu, Y.; Chen, Z.; Kanehira, M. Enhanced Chemical Stability of VO_2 Nanoparticles by the Formation of SiO_2/VO_2 Core/Shell Structures and the Application to Transparent and Flexible VO_2-Based Composite Foils with Excellent Thermochromic Properties for Solar Heat Control. *Energy Environ. Sci.* **2012**, *5*, 6104–6110.
40. Gao, Y.; Cao, C.; Dai, L.; Luo, H.; Kanehira, M.; Ding, Y.; Wang, Z. L. Phase and Shape Controlled VO_2 Nanostructures by Antimony Doping. *Energy Environ. Sci.* **2012**, *5*, 8708–8715.
41. Kim, H.; Kim, Y.; Kim, T. Y.; Jang, A.-R.; Jeong, H. Y.; Han, S. H.; Yoon, D. H.; Shin, H. S.; Bae, D. J.; Kim, K. S.; *et al.* Enhanced Optical Response of Hybridized VO_2/Graphene Films. *Nanoscale* **2013**, *5*, 2632–2636.
42. Lee, C.-H.; Kim, Y.-J.; Hong, Y. J.; Jeon, S.-R.; Bae, S.; Hong, B. H.; Yi, G.-C. Flexible Inorganic Nanostructure Light-Emitting Diodes Fabricated on Graphene Films. *Adv. Mater.* **2011**, *23*, 4614–4619.
43. Sato, T.; Sato, I. Requirement Governing Light Sources Used for Color Evaluation. *Proceedings of the 8th Congress of the International Colour Association*; Kyoto, Japan, May 25−30, 1997; Vol. 1, pp 415−418.